Electronic Supplementary Material (ESI) for Journal of Materials Chemistry A.
This journal is © The Royal Society of Chemistry 2023

Supporting Information

Role of the electrode-edge in optically sensitive three-dimensional carbon foam-MoS_2 based high-performance micro-supercapacitors

Sumana Kumar[a], Anwesha Mukherjee[a], Swanand Telpande[b], Ayon Das Mahapatra[a], Praveen Kumar[b], Abha Misra[*a]

[a]Department of Instrumentation and Applied Physics, Indian Institute of Science, Bangalore, Karnataka 560012, India. E-mail: abha@iisc.ac.in

[b]Department of Materials Engineering, Indian Institute of Science, Bangalore, Karnataka 560012, India

*Corresponding author, Email: abha.misra1@gmail.com

Calculations

The gravimetric capacitances ($C_S, F/g$) were calculated from the CV curve at different scan rates by the equation,[1]

$$C_S = \frac{\int IdV}{mv\Delta V} \quad (1)$$

Where, $\int IdV$ denotes the area under the CV curve, m is the mass of active material of the working electrode (g), v is the scan rate (V/s), and ΔV is the operating potential range (V).

The gravimetric capacitance ($C_S, F/g$) was evaluated from the CD curve using the following equation, [2]

$$C_S = \frac{I\Delta t}{m\Delta V} \quad (2)$$

Where, I is the discharge current (A) and Δt is the discharge time (s) after the voltage (IR) drop.

The areal specific capacitances ($C_A, F/cm^2$) were calculated from the CV curves using the following equation,[2]

$$C_A = \frac{\int IdV}{Av\Delta V} \quad (3)$$

Where, A is the entire device area including electrodes and the gap between the electrodes (cm^2).

The volumetric capacitances ($C_V, F/cm^3$) were calculated from the CV curves using the equation,

$$C_V = \frac{C_A}{d} \quad (4)$$

Where, d is the thickness of coated material on electrodes (cm).

The energy ($E_A, Wh/cm^2$) and power density ($P_A, W/cm^2$) of the devices were evaluated by the following equations, respectively.[2]

$$E_A = \frac{1}{2} \times C_A \times \frac{(\Delta V)^2}{3600} \quad (5)$$

$$P_A = \frac{E_A}{\Delta t} \times 3600 \quad (6)$$

Where, Δt is the discharge time (s).

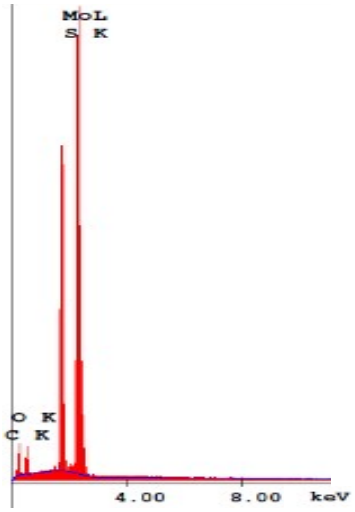

Element	Weight %	Atomic %
C K	19.83	47.77
O K	6.99	12.65
Mo L	44.05	13.29
S K	29.13	26.29

Figure S1: EDX spectrum of CF-MoS_2 composite.

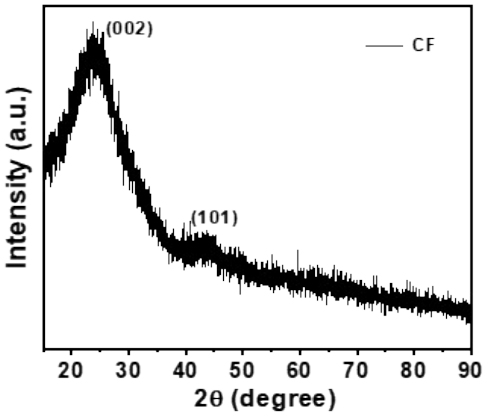

Figure S2: XRD pattern of CF.

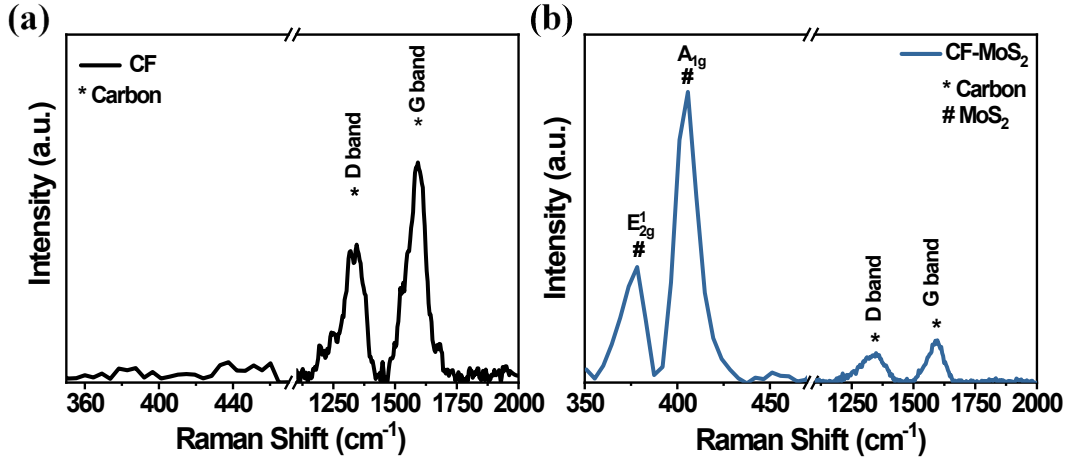

Figure S3. Raman spectra of (a) CF and (b) CF-MoS_2.

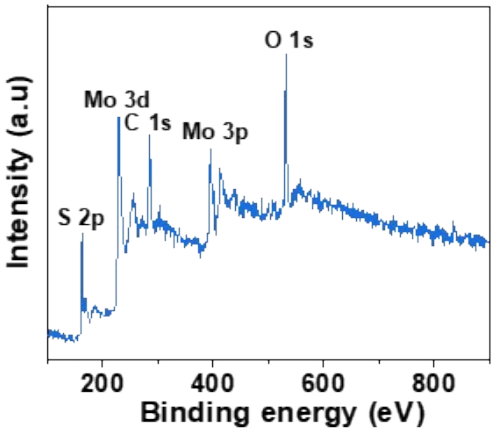

Figure S4: XPS survey spectra of CF-MoS_2 hybrid.

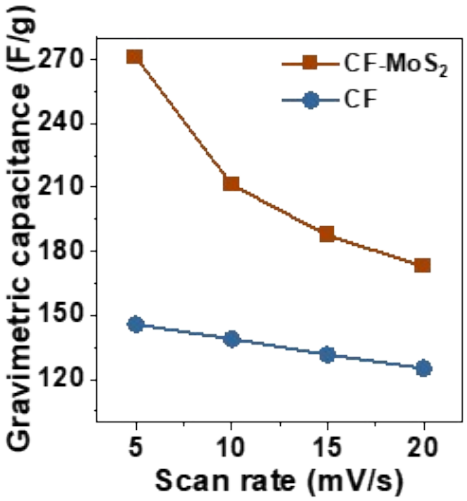

Figure S5: Gravimetric capacitance as a function of scan rates for CF-MoS_2 hybrid and CF.

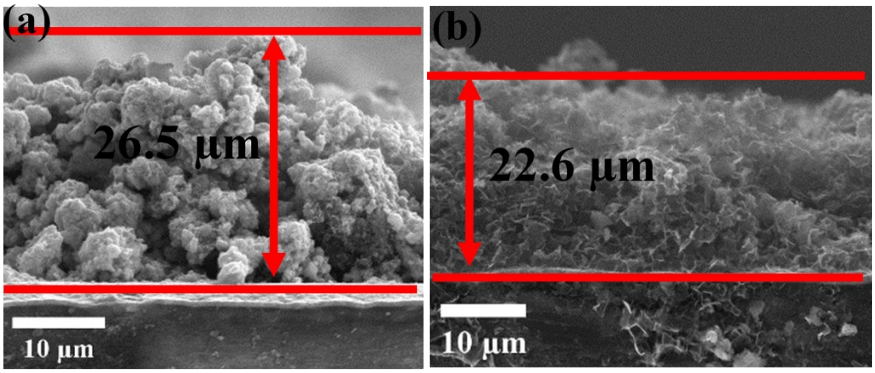

Figure S6: Cross-sectional SEM image of (a) CF-MoS_2 composite and, (b) CF coated working electrodes.

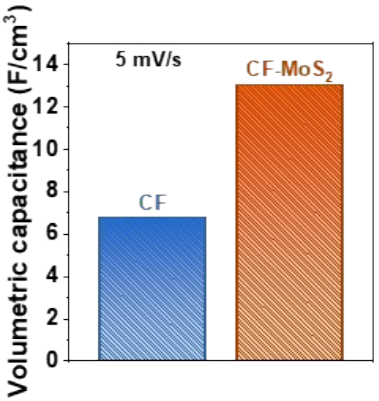

Figure S7: Comparison of volumetric capacitance of CF and CF-MOS_2 at a scan rate of 5 mV/s.

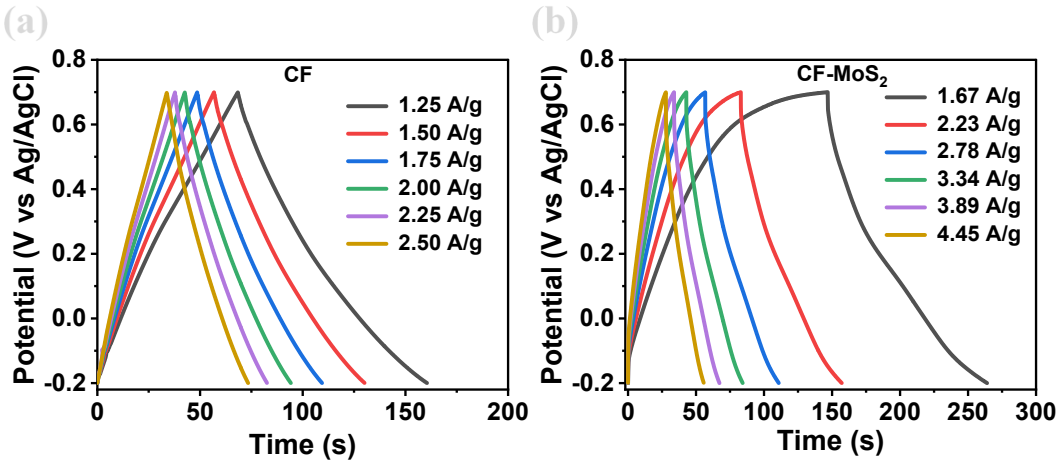

Figure S8: CD curves of (a) CF and (b) CF-MoS_2 electrode at various current densities.

Table S1: Gravimetric capacitance comparison of CF-MoS_2 with reported nanostructured MoS_2 and MoS_2-based composites.

MoS_2 material	**Method of preparation**	**Electrochemical properties**	**Reference**
MoS_2/rGO	Microwaves	148 F/g at 10 mV/s	[3]
MoS_2 nanosheets	Hydrothermal	129.2 F/g at 1A/g	[4]
MoS_2 nanostructure	Hydrothermal	106 F/g at 5mV/s	[5]
MoS_2 microspheres	Biopolymer-assisted Hydrothermal	185 F/g at 1 A/g	[6]
C/MoS_2 nanocomposites	Hydrothermal	210 F/g at 1 A/g	[7]
MoS_2/RCF composite	Hydrothermal	214.8 at 1 A/g	[8]
MoS_2/C composite	Hydrothermal	201.4 F/g@ 0.2 A/g	[9]
MoS_2-titanium plate	Hydrothermal	133 F/g@ 1A/g	[10]
Yolk-shell MoS_2 microsphere	Hydrothermal	161.4 F/g at 1 A/g	[11]
CF-MoS_2	Hydrothermal	270 F/g at 5 mV/s 226 F/g at 1.6 A/g	This work

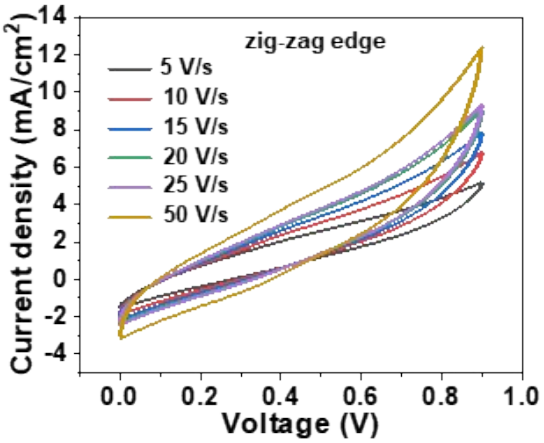

Figure S9: CV curves of CF-MoS_2 material coated zig-zag electrode based micro-supercapacitors at high scan rates ranging from 5 to 50 V/s.

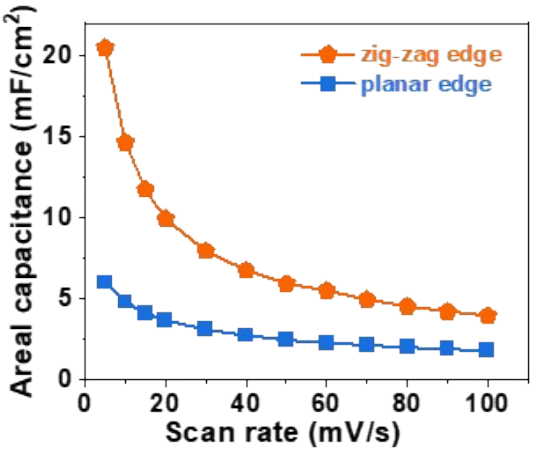

Figure S10: Areal specific capacitance calculated from CV curves at different scan rates ranging from 5 to 100 mV/s.

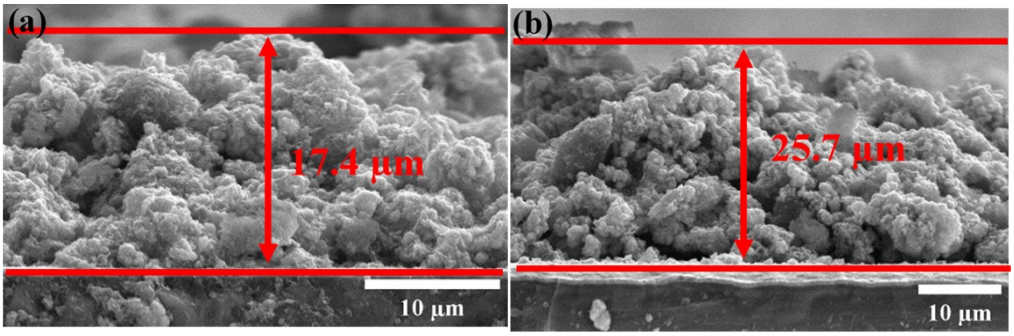

Figure S11: Cross-sectional SEM image of (c) CF-MoS_2 composite coated zig-zag electrodes, (d) CF-MoS_2 composite coated interdigitated electrodes.

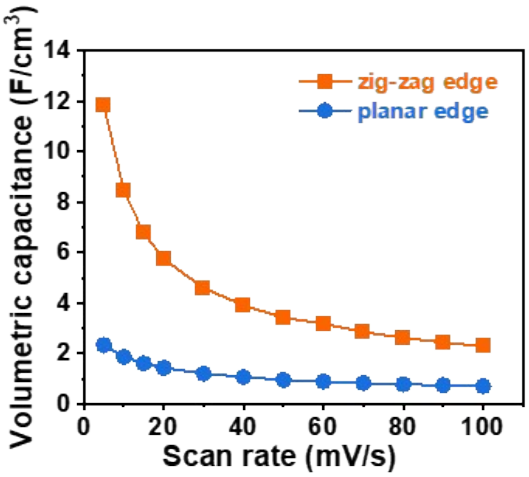

Figure S12: Volumetric capacitance calculated from CV curves at different scan rates ranging from 5 to 100 mV/s.

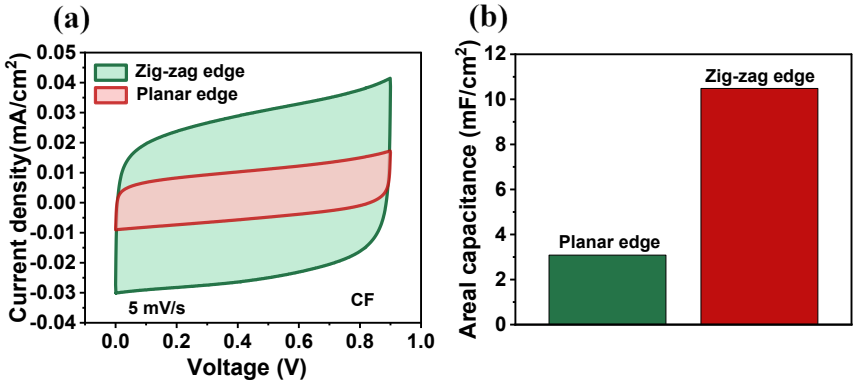

Figure S13: (a) CV responses and (b) comparison of areal specific capacitance with zig-zag edge and planar edge electrodes using CF as electrode material at a scan rate of 5 mV/s.

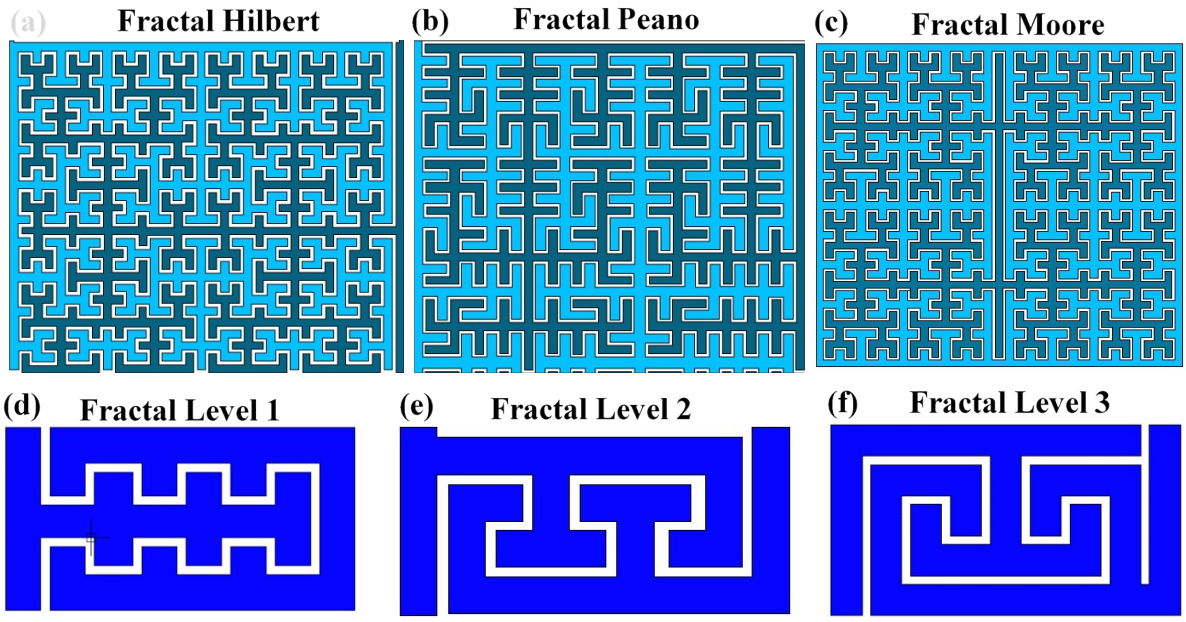

Figure S14: Schematics of different type of Fractal electrode geometry ((a)-(c): adapted from previous reference[12] and (d)-(f): adapted from previous reference[13]).

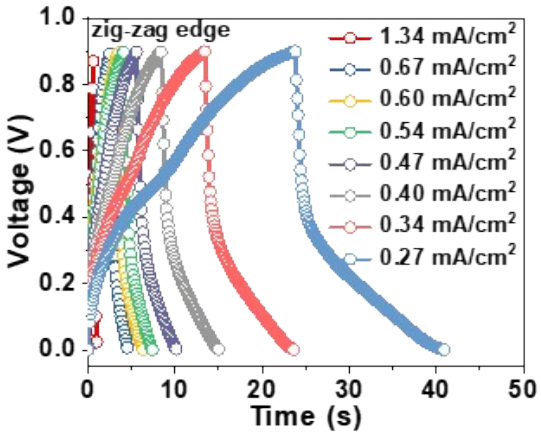

Figure S15: Charge-discharge curves of zig-zag edge electrode based micro-supercapacitors at different applied current densities.

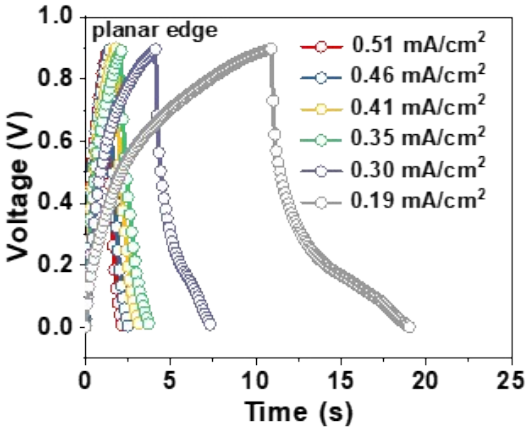

Figure S16: Charge-discharge curves of planar edge electrode based micro-supercapacitors at different applied current densities.

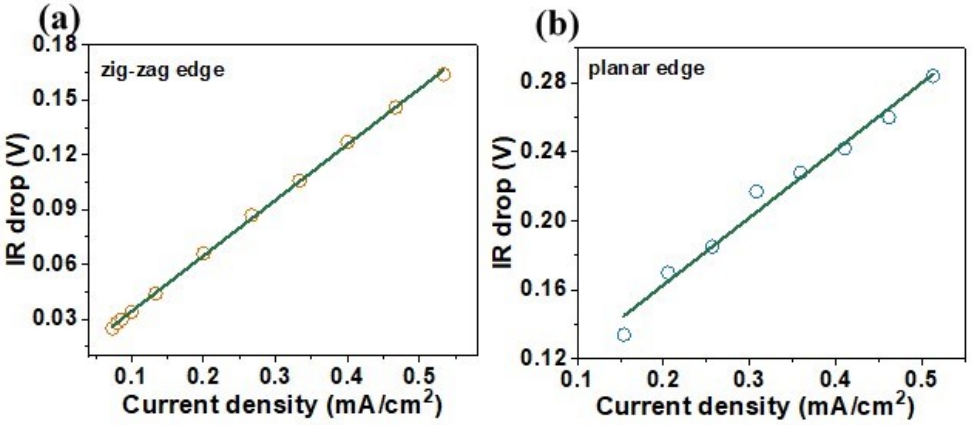

Figure S17: (a) The voltage drop (IR drop) associated with zig-zag micro-supercapacitor versus different current densities. (b) The voltage drop (IR drop) is associated with planar edge micro-supercapacitor versus different current densities.

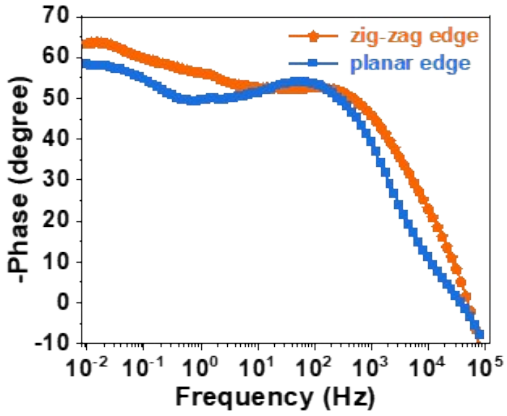

Figure S18: Bode plot of zig-zag edge and planar edge micro-supercapacitors.

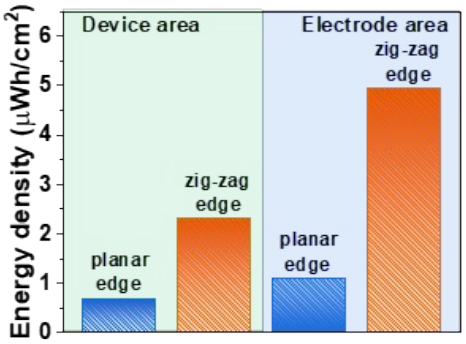

Figure S19: Ragone plot of the zig-zag edge and planar edge micro-supercapacitors calculated from CV curve, considering total area of the device and area of the electrodes (excluding gap between the fingers) at a scan rate of 5 mV/s.

Table S2: Capacitance retention comparison of zig-zag edge micro-supercapacitor with reported micro-supercapacitors.

Micro-supercapacitor structure	**Electrolyte**	**Retention**	**Reference**
MoS_2 film	aqueous electrolytes	92%(1000)	[14]
MoS_2/RGO	1 M $HClO_4$	92% (1000)	[3]
MoS_2/polypyrrole(PPy)	1 M KCl	85% (4000)	[15]
3D PEDOT:PSS/graphene	PVA/H_2SO_4	88.6%(5000)	[16]
GP/PANI-G/GP	PVA/H_2SO_4	80.9%(5000)	[17]
PEDOT	PVA/LiCl	96.6%(5000)	[18]
MoS_2-rGO hybrid	PVA/H_2SO_4	88.6% (5000)	[19]
Inkjet printed MoS_2	PVA/ H_2SO_4	85.6%10000)	[20]
MXene/graphene aerogels	6 M KOH	90% (10000)	[21]
MXene	PVA/Na_2SO_4	91.4%(10000)	[22]
MnO_x/Au	1 M Li_2SO_4	74.1%(15000)	[23]
MoS_2/nanoporous graphene film	PVA/H_3PO_4	82.2%(20000)	[24]
CF-MoS_2	**PVA/H_2SO_4**	**96.2%(5000)**	**This work**

Table S3: A comparison of the perimeter to surface area ratio for different electrode designs.

Electrode geometry	**Change in perimeter-to-surface area ratio compared to IDE (%)**	**Reference**
Fractal Moore	30.46	[12]
Fractal Peano	26	[12]
Fractal Hilbert	39.5	[12]
Zig-Zag edge	50	This work

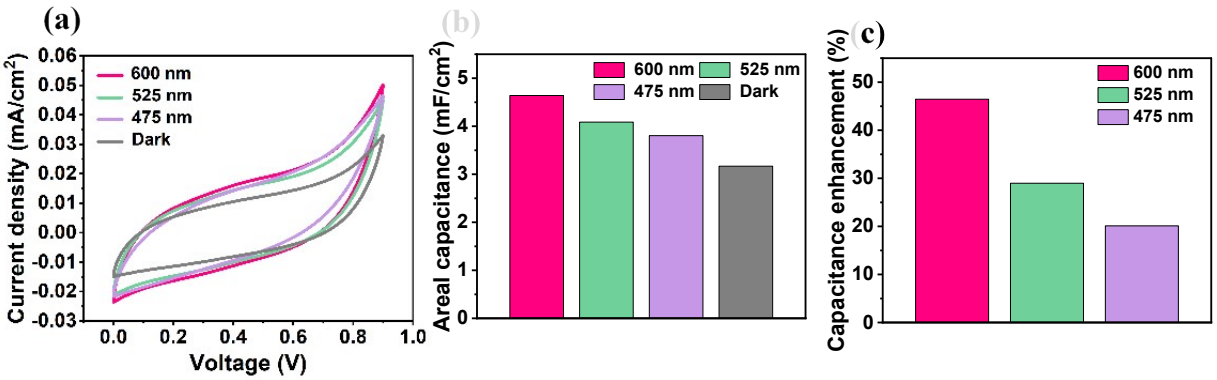

Figure S20: (a) CV curves in dark and under illumination using wavelengths of 600 nm, 525 nm, and 475 nm at a scan rate of 5 mV/s. (b) Areal capacitance comparison in dark and under illumination (600 nm, 525 nm, and 475 nm) obtained from CV. (c) Capacitance enhancement under illumination using 600 nm, 525 nm, and 475 nm in comparison with the dark condition.

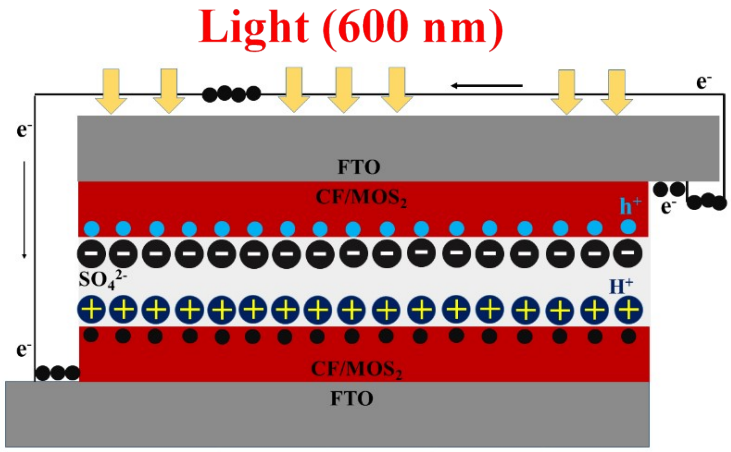

Figure S21: Schematic of CF-MOS_2/FTO device in photo-recharged condition.

References

1 Z. Fan, J. Yan, T. Wei, L. Zhi, G. Ning, T. Li and F. Wei, *Adv. Funct. Mater.*, 2011, **21**, 2366–2375.

2 J. Li, S. Sollami Delekta, P. Zhang, S. Yang, M. R. Lohe, X. Zhuang, X. Feng and M. Östling, *ACS Nano*, 2017, **11**, 8249–8256.

3 E. G. Da Silveira Firmiano, A. C. Rabelo, C. J. Dalmaschio, A. N. Pinheiro, E. C. Pereira, W. H. Schreiner and E. R. Leite, *Adv. Energy Mater.*, 2014, **4**, 1–8.

4 K. J. Huang, J. Z. Zhang, G. W. Shi and Y. M. Liu, *Electrochim. Acta*, 2014, **132**, 397–403.

5 K. Krishnamoorthy, G. K. Veerasubramani, S. Radhakrishnan and S. J. Kim, *Mater. Res. Bull.*, 2014, **50**, 499–502.

6 L. Ma, L. M. Xu, X. P. Zhou and X. Y. Xu, *Mater. Lett.*, 2014, **132**, 291–294.

7 B. Hu, X. Qin, A. M. Asiri, K. A. Alamry, A. O. Al-Youbi and X. Sun, *Electrochim. Acta*, 2013, **100**, 24–28.

8 C. Zhao, Y. Zhou, Z. Ge, C. Zhao and X. Qian, *Carbon*, 2018, **127**, 699–706.

9 L. Q. Fan, G. J. Liu, C. Y. Zhang, J. H. Wu and Y. L. Wei, *Int. J. Hydrogen Energy*, 2015, **40**, 10150–10157.

10 L. Wang, Y. Ma, M. Yang and Y. Qi, *Appl. Surf. Sci.*, 2017, **396**, 1466–1471.

11 P. Wang, C. Zhou, B. Zheng, H. Liu, S. Sun and D. Guo, *Mater. Lett.*, 2018, **233**, 286–289.

12 M. K. Hota, Q. Jiang, Y. Mashraei, K. N. Salama and H. N. Alshareef, *Adv. Electron. Mater.*, 2017, 1700185.

13 K. H. Huang, C. Te Lin, Y. T. Chen and Y. J. J. Yang, J. Appl. Phys., 2019, 125, 014902.

14 L. Cao, S. Yang, W. Gao, Z. Liu, Y. Gong, L. Ma, G. Shi, S. Lei, Y. Zhang, S. Zhang, R. Vajtai and P. M. Ajayan, *Small*, 2013, **9**, 2905–2910.

15 H. Tang, J. Wang, H. Yin, H. Zhao, D. Wang and Z. Tang, *Adv. Mater.*, 2015, **27**, 1117–1123.

16 W. Yan, J. Li, G. Zhang, L. Wang and D. Ho, *J. Mater. Chem. A*, 2020, **8**, 554–564.

17 X. Shi, Z. S. Wu, J. Qin, S. Zheng, S. Wang, F. Zhou, C. Sun and X. Bao, *Adv. Mater.*, 2017, **29**, 1–9.

18 J. Wang, V. K. Bandari, D. Karnaushenko, Y. Li, F. Li, P. Zhang, S. Baunack, D. D. Karnaushenko, C. Becker, M. Faghih, T. Kang, S. Duan, M. Zhu, X. Zhuang, F. Zhu, X. Feng and O. G. Schmidt, *ACS Nano*, 2019, **13**, 8067–8075.

19 C. Yu, H. Xu, Y. Sun, X. Zhao, Z. Hui, Y. Gong, R. Chen, Q. Chen, J. Zhou, G. Sun and W. Huang, *Carbon*, 2020, **170**, 543–549.

20 B. Li, X. Liang, G. Li, F. Shao, T. Xia, S. Xu, N. Hu, Y. Su, Z. Yang and Y. Zhang, *ACS Appl. Mater. Interfaces*, 2020, **12**, 39444–39454.

21 X. Tang, H. Zhou, Z. Cai, D. Cheng, P. He, P. Xie, D. Zhang and T. Fan, *ACS Nano*, 2018, **12**, 3502–3511.

22 Y. Xie, H. Zhang, H. Huang, Z. Wang, Z. Xu, H. Zhao, Y. Wang, N. Chen and W. Yang, *Nano Energy*, 2020, **74**, 104928.

23 W. Si, C. Yan, Y. Chen, S. Oswald, L. Han and O. G. Schmidt, *Energy Environ. Sci.*, 2013, **6**, 3218–3223.

24 S. W. Kim, J. Hwang, S. J. Ha, J. E. Lee, J. C. Yoon and J. H. Jang, *J. Mater. Chem. A*, 2021, **9**, 928–936.